This is an open access article published under an ACS AuthorChoice License, which permits copying and redistribution of the article or any adaptations for non-commercial purposes.

Environmental Science & Technology

Article

pubs.acs.org/est

# Influence of Phytoplankton on Fate and Effects of Modified Zerovalent Iron Nanoparticles

Adeyemi S. Adeleye,*[†,‖,⊥] Louise M. Stevenson,[‡,‖,⊥] Yiming Su,[†,§,‖,⊥] Roger M. Nisbet,[‡,‖] Yalei Zhang,[§] and Arturo A. Keller*[†,‖]

[†]Bren School of Environmental Science & Management, University of California, Santa Barbara, California 93106-5131, United States

[‡]Department of Ecology, Evolution and Marine Biology, University of California, Santa Barbara, California 93106-5131, United States

[§]State Key Laboratory of Pollution Control and Resource Reuse, Tongji University, Shanghai 200092, China

[‖]University of California Center for Environmental Implications of Nanotechnology, Santa Barbara, California 93106-5131, United States

Supporting Information

**ABSTRACT:** Nanoscale zerovalent iron (nZVI) and its derivatives hold promise for remediation of several pollutants but their environmental implications are not completely clear. In this study, the physicochemical properties and aggregation kinetics of sulfide/silica-modified nZVI (FeSSi) were compared in algal media in which *Chlamydomonas reinhardtii* had been cultured for 1, 2, or 11 days in order to elicit the effects of organic matter produced by the freshwater algae. Furthermore, transformation of FeSSi particles were investigated in *C. reinhardtii* cultures in exponential (1-d) and slowing growth (11-d) phases while monitoring the response of algae. We found evidence for steric stabilization of FeSSi by algal organic matter, which led to a decrease in the particles' attachment efficiency. Transformation of FeSSi was slower in 11-d cultures as determined via inductively coupled plasma and X-ray analyses. High concentrations of FeSSi caused a lag in algal growth, and reduction in steady state population size, especially in cultures in exponential phase. The different outcomes are well described by a dynamic model describing algal growth, organic carbon production, and FeSSi transformations. This study shows that feedback from algae may play important roles in the environmental implications of engineered nanomaterials.

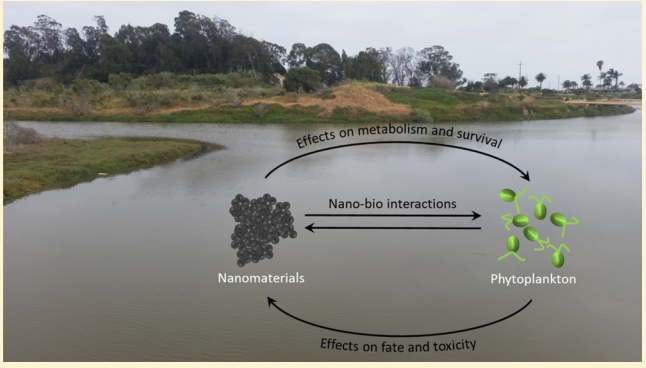


## 1. INTRODUCTION

Nanoscale zerovalent iron (nZVI) and its derivatives are emerging as an effective option for in situ treatment of important environmental contaminants such as heavy metals and chlorinated organic compounds.[1−4] Effective remediation of pollutants using nZVI in benchscale[2,5] and (mostly pilot) field studies[4,6−8] has been widely reported in the literature. However, our understanding of the environmental implications of these engineered nanomaterials (ENMs) drastically lags what we know about their potential applications.

nZVI aggregates in aqueous media due to low electrostatic repulsion and strong magnetic attraction between the particles,[9,10] limiting their mobility in the subsurface. Advances in nZVI-based technology include modifying the particles to prevent rapid aggregation and improve pollutant removal-capacity. Such modifications are done via surface-coating,[9,11] supporting them on other materials,[12,13] and doping them with other elements.[14−16] Improved mobility of nZVI increases their chances of reaching target contaminants as well as migration outside the treatment zone.[11,17,18] The removal capacity of some of these modified nZVI for certain pollutants is considerably higher than that of pristine particles (e.g., refs 16, 19, and 20), and the composites formed with pollutants after adsorption are more chemically stable than those formed by pristine nZVI.[16,20] As a result, we believe the use of modified nZVI will continue to increase.

The fate and effects of ENMs depend strongly on their physicochemical stability in the natural environment, which is mainly controlled by water chemistry.[10,21] However, natural waters also contain numerous microorganisms (bacteria and algae) that may interact with nanomaterials directly (through membrane-ENM interactions) or indirectly (e.g., via interactions between ENMs and microbial exudates).[22,23] It is still unclear how microorganisms and their exudates may influence the fate and effects of nZVI in natural waters. In this study, a modified nZVI (shown in a previous study to possess superior metal remediation and chemical stability)[20] was introduced into

Received: December 21, 2015
Revised: May 12, 2016
Accepted: May 16, 2016
Published: May 16, 2016

Downloaded via 207.241.234.15 on May 20, 2021 at 13:52:21 (UTC).
See https://pubs.acs.org/sharingguidelines for options on how to legitimately share published articles.



DOI: 10.1021/acs.est.5b06251
Environ. Sci. Technol. 2016, 50, 5597−5605

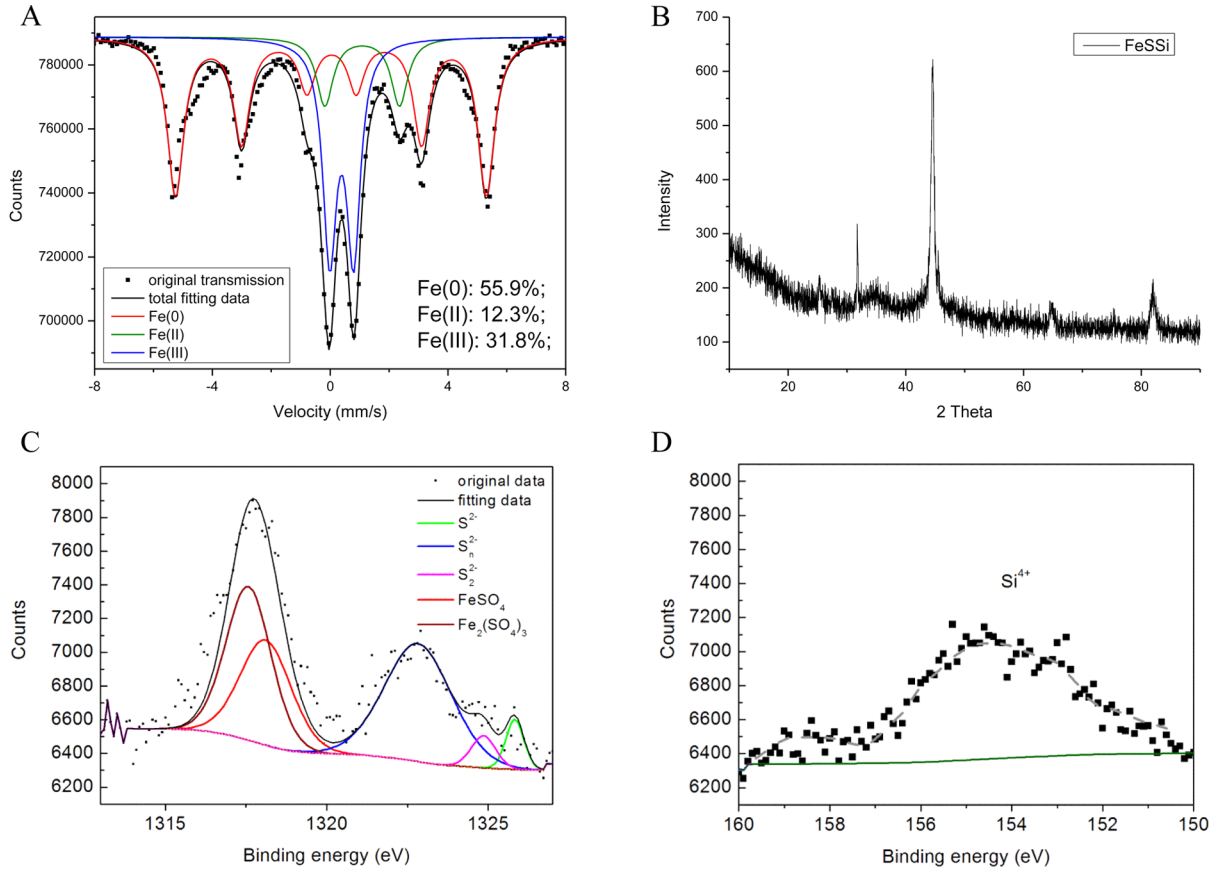


**Figure 1.** (A) Room-temperature Mössbauer analysis and (B) XRD diffractogram of FeSSi showing the state of Fe. XPS analyses of FeSSi show the chemical states of S (C) and Si (D). The R factor measure of goodness of fit (coefficient of determination) for Mössbauer analysis was 98.8%.

*Chlamydomonas reinhardtii* cultures in different stages of growth with the goal of investigating the influence of cells and/or their exudates on physicochemical properties, stability, transformation, and toxicity of the ENMs. We hypothesized that there will be a feedback between algae and the environmental impacts of ENMs.

## 2.0. MATERIALS AND METHODS

**2.1. Synthesis and Characterization of Modified nZVI.** Sulfide-modified nZVI seeded with silica (FeSSi) was synthesized as described in Su et al.[20] and summarized in the Supporting Information (SI) section S1.0. Major physicochemical properties of FeSSi were described previously.[20] Additional characterizations done in this study include Mössbauer spectroscopy, X-ray diffraction (XRD), and X-ray photoelectron spectroscopy (XPS) analyses to determine the bond states of the elements in FeSSi,[20] determination of initial hydrodynamic size (HDD) and zeta ($\zeta$) potential in deionized water using a Malvern Zetasizer Nano-ZS90,[22] as well as scanning electron microscopy (SEM, FEI XL30 Sirion). For the determination of HDD and $\zeta$ potential, the nanoparticle stock was bath-sonicated for 30 min (Branson 2510).

**2.2. Test Organism Cultures and Media.** Batch cultures of *C. reinhardtii* were grown in COMBO media (Table S1) as described previously.[24] Fresh cultures were inoculated to achieve a cell density of $10^6$ cells/mL and incubated at 20 °C (12:12 light/dark). To distinguish the effect of algal growth stage on the environmental implications of FeSSi, cultures of different ages (1, 2, and 11 days hereafter referred to as 1-d, 2-d, and 11-d, respectively) were used for the experiments. 2-d and 11-d cultures were obtained by inoculating fresh media to start batch cultures 1 or 10 days prior to the start of the experiment. 1-d cultures were inoculated on the day the experiment started. 1-d and 2-d cultures were in exponential phase while 11-d cultures were in slowing growth phase.[24]

**2.3. Culture Media and Characterization.** 1-d, 2-d, and 11-d media, with different amounts of algal organic matter (OM) were obtained from fresh COMBO media, 2-d, and 11-d cultures, respectively, and characterized. A description of how the media were obtained and characterized is provided in section S2.0. Sterile COMBO media was used as 1-d media to clearly see the effect of algal-derived OM.

**2.4. Effect of Algal Organic Matter on Stability of FeSSi.** The HDD and $\zeta$ potential of FeSSi (50 mg/L) were measured in 1-d, 2-d, and 11-d media using the Zetasizer. Aggregation kinetics and attachment efficiency of FeSSi ($\alpha$) were also studied in the three media via dynamic light scattering (DLS) as described previously,[21,22] and summarized in section S3.0.

**2.5. Influence of Algae on Dissolution and Effect of FeSSi.** To study transformation and effects of FeSSi in freshwater environments, stock suspensions of the nanoparticles were added to 1-d and 11-d media (without the organisms) and mixed thoroughly for 1 h (80 rpm, Dayton-6Z412A roller-mixer) to allow direct interactions between FeSSi and algal OM. The mixed stocks were respectively used to dose 1-d or 11-d cultures (with the organisms) in triplicates to achieve final FeSSi concentrations of 1.8, 18, and 180 mg/L. We intentionally used concentrations lower than what is typically injected into the subsurface, 1−30 g/L,[6] in order to


DOI: 10.1021/acs.est.5b06251
Environ. Sci. Technol. 2016, 50, 5597−5605

Table 1. Hydrodynamic Size, Zeta Potential, and Attachment Efficiency of FeSSi in Media

| media | hydrodynamic size (nm) | Zeta potential (mV) | attachment efficiency, $\alpha$ |
|---|---|---|---|
| DI water[a] | 341 | −38.0 | 0.07 |
| day 1 (1-d) media | 369 | −17.0 | 0.18 |
| day 2 (2-d) media | 392 | −17.3 | 0.21 |
| day 11 (11-d) media | 390 | −11.4 | 0.09 |

[a]Contained pH 7.5 phosphate buffer (Ionic strength = 13.4 mM).

account for mass loss during transport from points of injection into nearby surface waters. To monitor dissolution, aliquots were carefully taken at time points from the supernatant, filtered (0.45 $\mu$m) to remove cells and particles, digested with trace-metal grade $HNO_3$ (Fisher Scientific), and analyzed for iron, silicon, and sulfur via ICP-AES (Thermo Scientific iCAP 6300). FeSSi particles aggregate in algal media to sizes greater than 0.45 $\mu$m within 3 min and are thus not expected to pass through the filter. The effect of FeSSi on algal population density over time was monitored by measuring concentrations of chlorophyll a (Gemini XPS Fluorescence Microplate Reader). Fluorescence was converted to concentrations of chlorophyll a ($\mu$g/L) using a standard curve made with Turner Designs Liquid Primary Chlorophyll a Standards.[24]

A process-based, dynamic model adapted from Stevenson et al.[24] was used to describe the response of *C. reinhardtii* to FeSSi in this study. The FeSSi-algal model (described fully in section S4.0) includes phytoplankton growth, dissolved organic carbon (DOC) production, the concentration of "bioavailable" or toxic FeSSi particles and "inactivated" FeSSi particles (Table S3). We chose between model variants using a Likelihood Ratio Test[25] and fit parameters to algal biomass (chlorophyll a values) and DOC data (see model details and the fit to DOC data in section S4.0).

**2.6. Transformation of FeSSi.** To study particle transformation, stock of FeSSi suspension in 1-d and 11-d media (mixed for 1 h) was added to 1-d and 11-d cultures, respectively, to achieve 180 mg/L. Solid fractions (which include FeSSi and algal cells) were separated from the aqueous phase, and analyzed (over 30 d) via X-ray diffraction (XRD, Bruker D8 Advance) and X-ray photoelectron spectroscopy (XPS, Kratos Axis Ultra). To prepare the sample, the solid fractions were separated from suspension via centrifugation (10 000*g*, 30 min). Particles were immediately dried under vacuum (Yamato ADP-21) after decanting the supernatant. Interactions between FeSSi and algal cells were visualized using a Phillips FEI XL30 FEG environmental SEM as described in section S5.0.

## 3.0. RESULTS AND DISCUSSION

**3.1. Particle and Media Characterizations.** A representative SEM image of FeSSi with surface elemental composition is shown in Figure S3. Mössbauer spectroscopy showed that 56% of the total Fe in FeSSi was in the zerovalent ($Fe^0$) state (Figure 1a). As a reference, $Fe^0$ accounted for 60% of the total Fe in pristine nZVI synthesized in a manner similar to FeSSi (without the addition of dithionite and silica).[20] The other states of iron confirmed in FeSSi were $Fe^{3+}$ (32%) and $Fe^{2+}$ (12%). The presence of $Fe^0$ was confirmed by XRD analyses as shown by a strong peak at $2\theta$ = 44.5° (Figure 1b).[10,26] The presence of FeS in FeSSi was shown via X-ray absorption near edge structure (XANES) analyses in a previous study.[20] S 2p XPS spectrum (Figure 1c) shows that S on FeSSi surface exist as $S^{2-}$(4.1%), $S_2^{2-}$(3.6%), $S_n^{2-}$(36.2%), $FeSO_4$ (24.4%), and $Fe_2(SO4)_3$ (31.7%). Si exists mainly as $Si^{4+}$, as indicated by the peak located at 154 eV (Figure 1d). The isoelectric point (IEP) of FeSSi was determined as ∼pH 7.4 (Figure S4). The HDD of FeSSi in DI water (pH 7.5, 5 mM phosphate buffer), which is an average of DLS data collected over 2 min, was 341 nm. In the same conditions, the $\zeta$ potential of FeSSi was −38.0 mV, which is much higher than one would expect at a pH ≈ IEP. The high negative charge under this condition is probably due to the adsorption of phosphate ions from the buffer by FeSSi. Although the $\zeta$ potential value suggests stability, FeSSi particles aggregated to ∼470 nm within 6 min after which they were relatively stable (Figure S5).

Major properties of the media used in this study are presented in Table S4. DOC, which is a proxy for algal OM and dissolved oxygen (DO) in media, increased with culture age while nitrogen and phosphorus decreased over time as they were used up by cells. We also observed that pH increased from 7.6 to ∼10 in 11-d media because COMBO media is typically unbuffered. The major functional groups in algal OM are shown in Figure S6 and detailed band assignments are provided in Table S5.

**3.2. Effect of Algal Organic Matter on Stability of FeSSi.** The initial size of FeSSi in 1-d media (pH 7.6, HDD = 369 nm) was slightly larger than (though not significantly $p$ = 0.41) in buffered DI with similar pH (pH 7.5, HDD = 341 nm). This suggests a slightly faster aggregation of FeSSi in 1-d algal media than in DI. The ionic strength (IS) of 1-d media, calculated from the composition of COMBO media as ∼5.41 mM, is much lower than the IS of DI due to phosphate buffer (∼13.4 mM). One reason for a lower stability of FeSSi in 1-d media is the significantly lower ($p = 1.5 \times 10^{-6}$) surface charge ($\zeta$ potential = −17.0 mV) compared to DI ($\zeta$ potential = −38.0 mV). 1-d media contained multivalent ions such as $Ca^{2+}$, $Mg^{2+}$, etc., which are able to screen the electrostatic layer of colloids more strongly than the monovalent cations ($Na^+$) in buffered DI.

In 11-d media, the initial size of FeSSi was larger (HDD = 390 nm); however, aggregation kinetics showed that FeSSi did not aggregate as fast in this condition relative to 1-d and 2-d media (Table 1, Figure S5). A previous study concluded that such increase in initial size of the nanoparticles that could not be attributed to faster aggregation was indicative of particle coating.[22] The $\zeta$ potential of FeSSi was significantly less negative in 11-d media (−11.4 mV) than DI and 1-d media ($p = 9.7 \times 10^{-6}$ and $2.9 \times 10^{-5}$, respectively). Despite this low surface charge in 11-d media, the attachment efficiency of FeSSi was comparable to what we found in DI, and much lower than in 1-d and 2-d media (Table 1).

Slower aggregation of FeSSi in 11-d media could not be attributed to lower ionic content as conductivity was slightly higher in 11-d media than in 1-d and 2-d media (Table S4). We therefore hypothesized that slower aggregation of FeSSi in 11-d media was due to high pH and/or steric stabilization by algal OM. As reported earlier, 11-d media had a pH of ∼10


DOI: 10.1021/acs.est.5b06251
Environ. Sci. Technol. 2016, 50, 5597−5605

compared to pH ~ 7.6 found in 1-d and 2-d media. nZVI, and ENMs in general, are typically more negatively charged at higher pH which may improve their stability via increased electrostatic repulsion.[16,27] To confirm the contribution of pH to improved stability of FeSSi in 11-d media, the aggregation kinetics of FeSSi was also studied in 11-d media whose pH was adjusted to 7.6 using dilute HCl. The mean HDD of FeSSi over 1 h in pristine 11-d media (649 nm) was statistically similar ($p = 0.06$) to measurements performed in pH-adjusted 11-d media (627 nm, Figure 2). In addition, attachment efficiency was

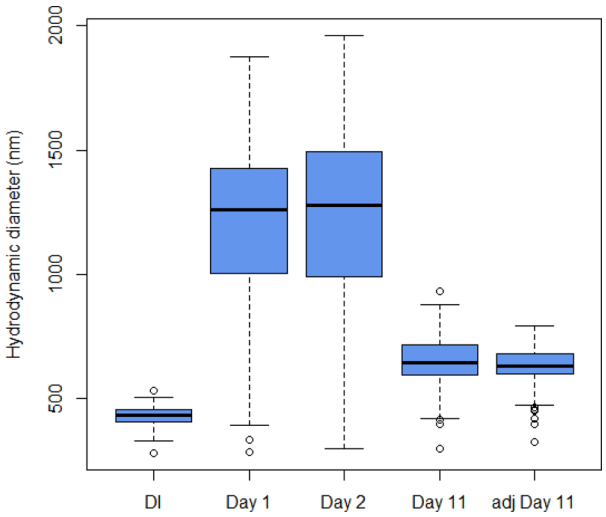


**Figure 2.** Tukey boxplot of hydrodynamic size distribution of FeSSi in 1-d (Day 1), 2-d (Day 2), 11-d (Day 11), and pH adjusted 11-d (adj Day 11) media over 1 h.

slightly lower in adjusted 11-d media ($\alpha = 0.08$) than in pristine 11-d media ($\alpha = 0.09$). This implies that higher pH did not contribute substantially to improved stability of FeSSi in 11-d media. On the basis of (1) this insensitivity of FeSSi stability to pH in 11-d media, (2) improved stability of FeSSi in 11-d media compared to 1-d and 2-d media despite having a much less-negative $\zeta$ potential, and (3) increase in the initial size of FeSSi in 11-d media which was not due to increased aggregation, we concluded that slower aggregation of the nanoparticles in 11-d media was rather due to their coating by algal OM, which provided steric stabilization.

The organic matter of microorganisms is mostly composed of extracellular polymeric substances or EPS, and is abundant in natural environments.[28,29] EPS are made up of a wide range of macromolecules such as polysaccharides, proteins, glycolipids, nucleic acids, phospholipids, and other polymeric substances excreted by microorganisms,[28,30] which may be held together by electrostatic interactions, hydrogen bonds, London dispersion forces, ionic interactions, and chain−chain complex networks.[31,32] These polymers contain charged functional groups such carboxyl, amine, and phosphate, etc. (Figure S6) which can interact with other charged surfaces in aqueous media, including ENMs.[21,22,29,31,33] In addition, EPS contain hydrophobic polysaccharides,[30] which can interact with other hydrophobic surfaces. The interactions of EPS with nanomaterials were shown to impart stability to carbon nanotubes,[21] copper-based nanoparticles,[22] ferrihydrite,[29] and Fe-containing dust nanoparticles.[29]

**3.3. Influence of Algae on Transformation of FeSSi.** nZVI reacts with oxygen in water to produce ferrous ions ($Fe^{2+}$), which may undergo oxidation to form ferric ions ($Fe^{3+}$).[10] $Fe^{3+}$ tends to precipitate on the surface of particles to form ferric oxide or oxohydroxide, especially at high pH.[10,27] FeSSi, which is black in its pristine state, turned rusty brown within 1 h of mixing in 1-d media, while it remained mostly black in 11-d media (Figure S7). This visual observation supports the analytical data provided in the following section, which clearly show that FeSSi is transformed in these aqueous systems, much more so in the 1-d media conditions.

*3.3.1. Aqueous Phase.* In order to determine how the presence of algae affects dissolution of FeSSi, we monitored concentrations of dissolved iron ($[Fe]_{diss}$), silicon ($[Si]_{diss}$), and sulfur ($[S]_{diss}$), all components of FeSSi, in 1-d and 11-d *C. reinhardtii* cultures. $[Fe]_{diss}$ was relatively low in all conditions (<0.3 mg/L, Figure S8) when compared to the concentrations of FeSSi introduced, which is probably due to fast oxidation of $Fe^{2+}$ ions to insoluble $Fe^{3+}$ species.[10] Nevertheless, the ratio of $[Fe]_{diss}$ in 1-d cultures with FeSSi to $[Fe]_{diss}$ in control cultures (measured 2 h after adding nanoparticles to cultures) was 1.86, 4.19, and 19.0 in treatments with 1.8, 18, and 180 mg-FeSSi/L, respectively. This ratio could not be determined for 11-d culture because $[Fe]_{diss}$ was nondetectable in control cultures by Day 7.

$[Fe]_{diss}$ in 11-d culture treatments was an order of magnitude lower relative to the corresponding 1-d culture conditions (Figure S8) which suggests a slower rate of $Fe^0$ oxidation in 11-d cultures despite the presence of a higher amount of DO (Table S4). Slower dissolution in 11-d culture may be due to algal OM coating of the particles, which may reduce the surface area available for dissolution and other reactions.[10,34] Slower oxidation in 11-d cultures may also be due to the presence of much higher algal population whose adsorption to FeSSi is hypothesized to reduce surface available for oxidation. A representative ESEM micrograph showing heteroaggregation between algae and FeSSi particles is shown in Figure 3.

Oxidation of $Fe^{2+}$ is typically faster at higher pH[35,36] but we observed that $[Fe]_{diss}$ decreased in 1-d culture at a much faster rate than in 11-d cultures, whose pH was much higher. For instance, at initial FeSSi concentration of 180 mg/L, $[Fe]_{diss}$

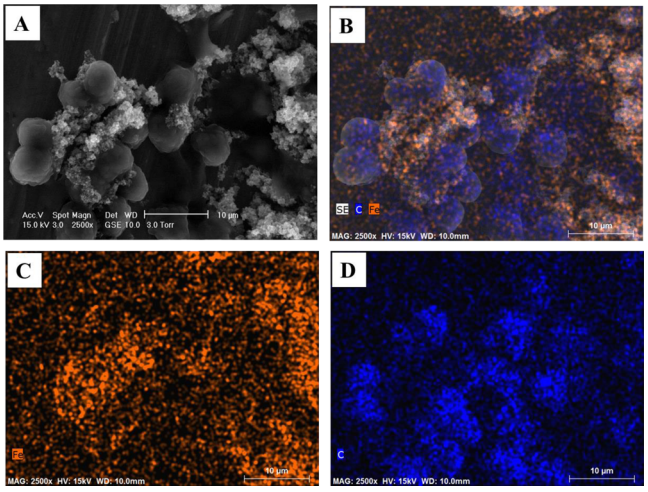


**Figure 3.** A representative ESEM micrograph with EDS hypermaps of 11-d culture with FeSSi particles. (A) Heteroaggregation between nanoparticle aggregates and *C. reinhardtii* cells, with (B) showing an overlay of carbon (C) and iron (Fe) distribution on micrograph. Individual hypermap of Fe is shown in (C) and C is shown in (D).


DOI: 10.1021/acs.est.5b06251
Environ. Sci. Technol. 2016, 50, 5597−5605

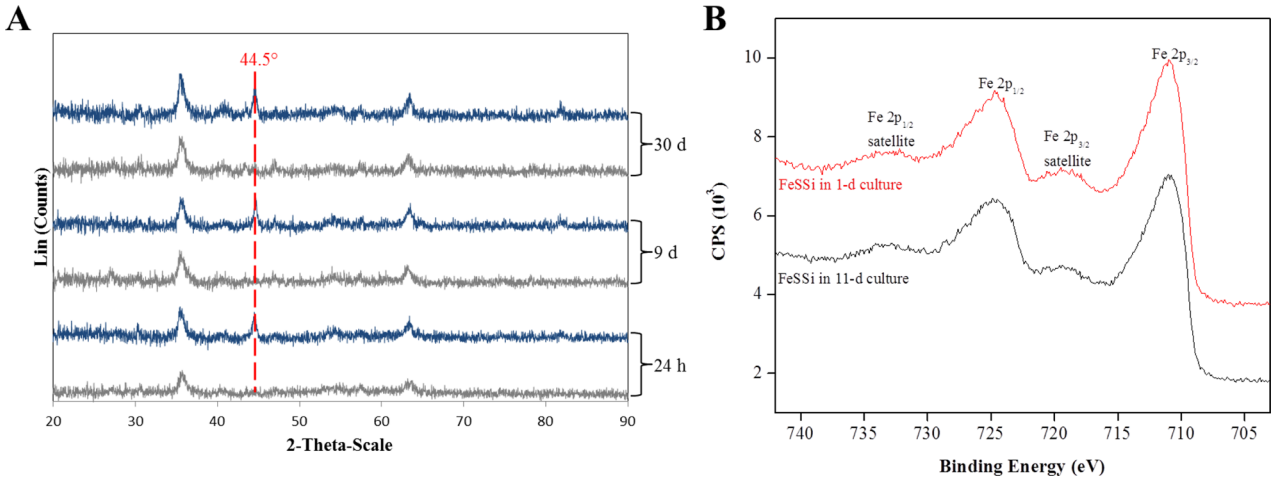


**Figure 4.** X-ray analyses of FeSSi in 1-d and 11-d cultures. (A) X-ray diffractograms of FeSSi (180 mg/L) in 1-d (gray) and 11-d (blue) media over 30 d, and (B) high resolution scans of Fe 2p in 1-d and 11-d cultures.

decreased by 170 and 7.26 ($\times 10^{-5}$ mg/L-h) within the first 96 h in 1-d and 11-d cultures, respectively. Slower oxidation of $Fe^{2+}$ is most likely due to the presence of higher amounts of algal OM in 11-d cultures (Figure S9), which binds to the ions and retards their oxidation. Gonzalez et al. recently reported slower rates of $Fe^{2+}$ oxidation with increasing amounts of algal exudates isolated from *Dunaliela tertiolecta*.[35] After 14 d of experiments, however, there was no obvious difference in the $[Fe]_{diss}$ levels in all the conditions.

The levels of $[S]_{diss}$ detected 2 h after adding FeSSi suspension was higher in all but one (that is, 1.8 mg-FeSSi/L in 11-d culture) FeSSi treatments compared to their respective controls. The highest initial increase in $[S]_{diss}$ was observed in the 180 mg-FeSSi/L conditions (48−52%). These results suggest leaching of S into cultures from FeSSi particles. $[S]_{diss}$ decreased with time in both the control and FeSSi treatment cultures, except at the highest FeSSi concentrations where we saw an increase in $[S]_{diss}$ over time probably due to continuous leaching of S from the particles (Figure S8). Release of S was faster in 11-d cultures than in 1-d cultures, probably due to higher size stability of the particles in the presence of algal OM, providing more surface area for dissolution. In contrast, $[Si]_{diss}$ detected 2 h after exposure of cultures to FeSSi was 1.8 > 18 > 180 mg-FeSSi/L in both 1-d and 11-d cultures; and lower than in control conditions in most cases. In fact, $[Si]_{diss}$ in 1-d and 11-d cultures exposed to 180 mg-FeSSi/L was lower by a factor of 2.9 and 3.5 relative to their respective control conditions. This trend suggests that FeSSi removed background Si from the aqueous phase. $Fe^0$ is known to have affinity for dissolved Si.[37] The adsorption properties of FeSSi may have important consequences in natural waters where the ENMs may adsorb to important nutrients.

*3.3.2. Solid Phase.* The XRD diffractograms showed peaks representing oxides of Fe in both 1-d and 11-d cultures in samples analyzed from 2 to 30 d. The major oxide peaks were assigned to $Fe_2O_3$, $\gamma$-$Fe_2O_3$, $Fe(OH)_3$, and $\gamma$-FeOOH. In addition, $Fe^0$ was detected in 11-d culture (corresponding to $2\theta = 44.5°$)[10,15] up to a month after exposure, but not in 1-d culture even after 48 h (Figure 4a). This implies that oxidation of FeSSi is slower in 11-d cultures, which supports our finding in the previous section where we reported that $[Fe]_{diss}$ was an order of magnitude higher in 1-d cultures than in 11-d cultures. Similarly, Liu and co-workers reported complete oxidation of nZVI in oxidized water within 48 h,[26] but we also show here that the presence of algal OM can slow down transformation of $Fe^0$ (in FeSSi) for a long period of time.

A comparison of the XPS spectra of 11-d culture with and without FeSSi showed evidence of removal of phosphorus from the aqueous phase by the particles (Figure S10, Table S6). The carbon/phosphorus (C/P) mass ratio (on Day 10) decreased from 153 when FeSSi was absent to 26 in the presence of FeSSi. Similarly, peaks for Ca (~348 eV) and Si (~153.5 eV) were observed in the XPS spectra of solid phase obtained when FeSSi was present, but not when FeSSi was absent. In fact, the amount of both elements detected in the solid phase increased over time, as can be determined by decrease in Fe/Ca and Fe/Si mass ratios over time. These results suggest that the bioavailability of some essential elements decreased in the presence of FeSSi, possibly due to adsorption onto the nanoparticles and/or (co)precipitation.

High resolution (HR) scan of Fe 2p was done in order to determine the chemical state of Fe at the surface of FeSSi. As shown in Figure 4b, there is no obvious difference between the HR spectra obtained from 1-d and 11-d cultures. The peak for $Fe^0$, typically at 707 eV,[38] was absent in all the spectra we obtained. However, we observed peaks for higher valent state of Fe around 711 eV, which may be assigned to either $Fe_2O_3$ or FeOOH based on features and peak positions.[26] A single peak is typically observed for O 1s of $Fe_2O_3$ (~530 eV),[26,39] but we observed double peaks for O 1s in this study (Figure S11). The Fe $2p_{3/2}$ and Fe $2p_{1/2}$ peaks located at 711.1 and 724.6, respectively, were thus assigned to FeOOH.[38,39] Our XPS analyses suggest that FeSSi was fully oxidized at the surface in both 1-d and 11-d cultures. The $Fe^0$ detected (via XRD) in FeSSi introduced into 11-d cultures was probably located in the core of nanoparticles, and it was not detected in 1-d cultures due to faster oxidation.

Our observation of slower oxidation in 11-d media is somewhat counterintuitive as one would expect a faster oxidation of $Fe^0$ in the slowing growth cultures, which have a higher amount of DO (Table S4).[40] The detection of $Fe^0$ in the core of FeSSi up to one month after exposure to 11-d cultures suggests that the influence of algal OM on $Fe^0$ oxidation is probably more important than the presence of DO in freshwater. Reinsch and co-workers had previously found that the presence of DO in aqueous media was probably more


DOI: 10.1021/acs.est.5b06251
Environ. Sci. Technol. 2016, 50, 5597−5605

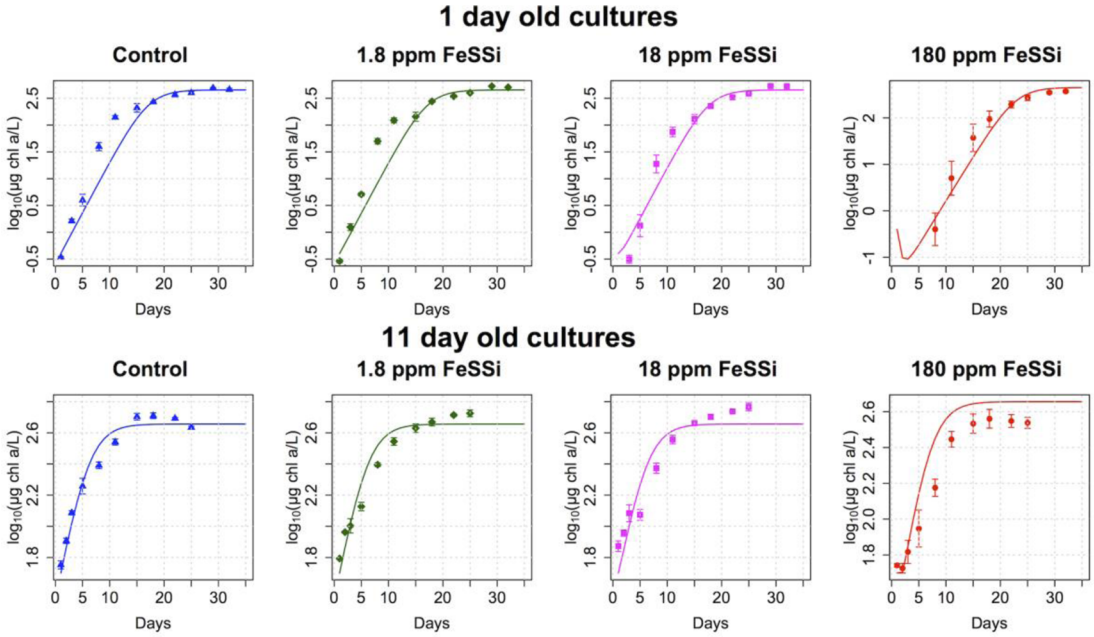


**Figure 5.** Fit of algal-FeSSi model to all algal treatments −1 and 11 day old cultures (in exponential and slowing growth phases, respectively) exposed to 0, 1.8, 18, and 180 mg-FeSSi/L. Error bars reflect the standard error of chlorophyll a concentrations between algal replicates ($n$ = 3 for all treatments). All seven parameters in Table S3 were estimated simultaneously for all treatments by fitting the model to observed chlorophyll a data (algal biomass) and DOC concentration measurements. Details in section S4.0.

important in $Fe^0$ oxidation than dissolved anions (which tend to inhibit oxidation).[40] Therefore, FeSSi (and other nZVI derivatives) may persist longer in productive natural waters where there may be an abundance of OM.

**3.4. Influence of Algae and Algal OM on Effects of FeSSi.** In order to investigate potential feedback between FeSSi and algal cells, we exposed algal cultures at exponential (1-d) and slowing growth (11-d) phases to 1.8, 18, and 180 mg-FeSSi/L. We observed a dose−response effect of FeSSi on cells (Figure 5 and Figure S12). Algal growth rate in 1-d cultures exposed to 1.8 and 18 mg-FeSSi/L was initially lower compared to controls but eventually grew to the same steady state population size as control cultures. In contrast, 11-d cultures did not exhibit any obvious negative effects to 1.8 and 18 mg-FeSSi/L. By the end of the experiment, 11-d cultures were 36 days old, and the control cultures had begun to decline probably due to cell senescence. However, 11-d cultures exposed to 1.8 and 18 mg-FeSSi/L may have reached a slightly higher steady state population size had the experiment continued, as they were still growing when the experiment ended.

While 1.8 and 18 mg-FeSSi/L did not have a strong effect in either growth stage, 180 mg-FeSSi/L had interesting effects on the algal cultures. 1-d cultures exposed to 180 mg-FeSSi/L declined immediately, such that the chlorophyll a was nondetectable within 2 h of dosing with FeSSi. These cultures remained below the detection limit until Day 7 of the experiment, after which cells grew exponentially to a slightly lower steady state algal population size than control cultures and cultures exposed to lower concentrations of FeSSi. If this had been an acute (48−96 h) toxicity study, then one would have considered FeSSi to have lethal effects on *C. reinhardtii* at 180 mg-FeSSi/L. This underscores the importance of (sub)-chronic toxicity studies over longer time periods in order to understand the long-term environmental effects of ENMs. 180 mg-FeSSi/L also had a clear effect on 11-d cultures, although the effect was less severe than to 1-d cultures. 11-d cultures initially declined in the first day of exposure to 180 mg-FeSSi/L and then grew at the same rate as the controls but reached a much lower steady state algal population size than control cultures and cultures exposed to lower concentrations of FeSSi.

Overall, the highest concentration of FeSSi had the most obvious effect on algal cultures in both stages of growth, and a greater effect on algal cultures exposed at an earlier stage of growth (Figure 5). This pattern is similar to the response of algal cultures in different growth phases to silver nanoparticles−silver nanoparticles were more toxic to algal cultures in earlier stages of growth than algae in later stages.[24] In that study, we discovered that the differential toxic response is due to the lower concentrations of DOC in earlier stages of growth compared to later stages.

The process-based, dynamic FeSSi-algal model broadly fits the response of the algae to FeSSi (Figure 5), notably the lag in growth of 1-d cultures exposed to 180 mg-FeSSi/L. With only 7 parameters, this model fits responses of algal biomass (chlorophyll a concentrations) and DOC (a proxy for algal OM) concentrations through time for all FeSSi and control treatments (Figures S1 and S2), although the fit to DOC for the highest FeSSi level is poor (see SI for possible explanations).

The model assumes that all of the FeSSi particles are toxic until they interact with DOC, and DOC mitigates the toxicity of the FeSSi particles by reducing bioavailability. The model does not describe the *mechanism* of DOC detoxification or of FeSSi toxicity. We now discuss two potential mechanisms: (1) reactive oxygen species (ROS) production by redox-active Fe species and subsequent ROS quenching by DOC and (2) binding of FeSSi by DOC that interrupts FeSSi toxicity that occur via close association to the algal cells.

Redox-active Fe species can produce reactive oxygen species (ROS) such as hydroxyl radical ($^{\bullet}OH$) and ferryl ion (Fe(IV)) via Fenton-type chemistry.[18,36] Electron-spin resonance (ESR)


DOI: 10.1021/acs.est.5b06251
Environ. Sci. Technol. 2016, 50, 5597−5605

spectroscopy showed that •OH is produced by FeSSi, more so than pristine nZVI (Figure 13). Oxidative stress typically affects algal growth and impairs photosynthesis via several mechanisms that have been extensively discussed in the literature.[18,41,42] This is probably the major toxicity mechanism of FeSSi to *C. reinhardtii* in this study. As we previously mentioned, $Fe^0$ in FeSSi was more reactive in 1-d media, which led to production of aqueous Fe (mostly $Fe^{2+}$) at concentrations an order of magnitude higher than in 11-d media. Both species ($Fe^0$ and $Fe^{2+}$), which are the most redox-active forms of iron,[18,42] must have produced ROS at levels that were toxic to algae. In 11-d cultures, however, reactivity of FeSSi was suppressed by algal OM, which may have also chelated some of the $Fe^{2+}$ produced as previously shown for other metals.[43] Data on the concentration of dissolved Fe also supports this hypothesis: by Day 7, $[Fe]_{diss}$ in 1-d cultures with 180 mg-FeSSi/L had decreased to levels similar to the initial $[Fe]_{diss}$ (i.e., Day 1) we found in 1-d cultures with 18 mg-FeSSi/L (<0.1 mg/L). Cells were probably able to recover as the amount of redox-active Fe species in aqueous phase decreased with time.

Organic matter (OM) is known to effectively scavenge ROS, especially the nonselective ones like •OH.[36,44] As such, less ROS may have been available in 11-d cultures, and algae could be better protected from ROS produced by redox-active Fe species in 11-d media than in 1-d media. Algal OM-chelated $Fe^{2+}$ was probably (eventually) bioavailable (as a source of Fe), which might explain the potentially larger steady state population of *C. reinhardtii* at 1.8 and 18 mg-FeSSi/L compared to control cultures where Fe was too low to be detected after 7 days.

As we showed in Figure 3, heteroaggregation occurred between algae and FeSSi particles in freshwater medium. In fact, aggregates of FeSSi were found to bridge *C. reinhardtii* cells. The attachments can lead to direct release of ROS to cell membrane, decrease in cell mobility, membrane lipid bilayer disruption, and decrease in nutrient flow between the cell and the external environment.[45] However, if algal OM bound with or covered the surface of the FeSSi particles (as shown earlier in section 3.2) such that it limited direct FeSSi-algal cell interactions, then this could also explain the pattern observed that 11-d cultures experienced less toxicity than 1-d cultures. Shading effects from FeSSi (including those bound by algal OM) may have contributed some toxicity especially at high exposure concentrations, but we believe this is minimal due to sedimentation of the nanoparticles.

## 4.0. ENVIRONMENTAL IMPLICATIONS

Exudates secreted by freshwater microorganisms will affect the stability of FeSSi (and possibly other ENMs) in surface waters. Once coated by the organic polymers, the surface properties of FeSSi (mainly surface charge) will change, and their aggregation will be slowed via steric stabilization. FeSSi will thus not settle out of the water matrix as fast as one would expect from particles with high attraction forces (van der Waals and magnetic interactions). This may lead to longer exposure of pelagic organisms. It is unclear if allochthonous organic matter (e.g., those released into water from degrading leaves) will have similar effects on FeSSi, and this needs to be studied.

Increase in media pH observed in this study may have some influence on the transformation of FeSSi and the metabolism of algae, which may not be as pronounced in natural waters where pH is largely buffered. For instance, transformation of $Fe^{2+}$ may be slower (since higher pH drives faster oxidation) leading to more bioavailable Fe. But also, the surface charge of FeSSi and algal OM may be less negative in natural waters, which may promote stronger electrostatic interactions. This will influence the stability of the nanoparticle, and probably lead to slower oxidation of FeSSi. Additional studies are thus needed to better understand how pH influences nanoparticle-algae interactions, and the findings of this study may only be carefully extrapolated to well-buffered systems. Further, the increase in pH could have impacted algal cell physiology, either by affecting algal metabolism directly or through availability of nutrients. However, the strength of our modeling approach outlined here is that altered algal growth with lower pH in buffered systems, if observed, can be incorporated into our mechanistic model by fitting algal growth and/or DOC production parameters to data on algae in natural waters, enabling our model to be used to predict the effects of FeSSi on natural environments.

In agreement with several previous studies we found that $Fe^0$ in FeSSi tends to oxidize rapidly in freshwater. But here, we show that in productive waters, which have a lot of organic matter, these nanoparticles may persist longer due to slower oxidation resulting from organic matter coating. Coating of FeSSi by microbial exudates will also have effect on its reactivity, adsorption properties, and toxicity. Transformation of FeSSi can lead to release of Fe and S into water. And as shown in this study, the adsorptive properties of the nanoparticles can also lead to removal of ions (e.g., phosphate, silicate, etc.) due to the near-neutral charges on the particle surface at environmental conditions. The adsorbed nutrients may be transformed on the surface of the particles to other forms that may or may not be available to organisms, or be released back into water as the particles transform further.

As shown here, long-term environmental impacts of FeSSi (and probably other ENMs) cannot be adequately predicted from acute toxicity studies as toxic effects of ENMs will change with their transformation in the environment. In addition, coating of FeSSi by algal exudates may strongly influence the toxicity of the nanoparticles, similar to a previous finding with silver nanoparticles. This environmental feedback between ENMs and algae need to be adequately accounted for in models used for evaluating the fate, transport, and ecological effects of ENMs.

## ■ ASSOCIATED CONTENT

### Supporting Information

The Supporting Information is available free of charge on the ACS Publications website at DOI: 10.1021/acs.est.5b06251.

Sections S1.0 and S2.0 showing aggregation kinetics of FeSSi and FeSSi-algal model. Tables S1−S6 showing the composition of COMBO media, dynamic model and parameters, media properties, FTIR band assignments, and composition of solid phases; Figures S1−S13 showing model fits, characterization of FeSSi and media, FeSSi aggregation kinetics, micrograph of cells after dosing, and X-ray and ESR spectra of FeSSi (PDF)

## ■ AUTHOR INFORMATION

### Corresponding Authors

*Tel: (+1)805-893-5352; fax: (+1)805-893-7612; e-mail: adeyemiadeleye@umail.ucsb.edu (A.S.A.).

*Tel: (+1)805-893-7548; fax: (+1)805-893-7612; e-mail: keller@bren.ucsb.edu (A.A.K.).



DOI: 10.1021/acs.est.5b06251
Environ. Sci. Technol. 2016, 50, 5597−5605

### Author Contributions

[⊥]A.S.A., L.M.S., and Y.S. contributed equally to this work.

### Notes

The authors declare no competing financial interest.

## ■ ACKNOWLEDGMENTS

This material is based upon work supported by the NSF and the EPA under Cooperative Agreement Number DBI 0830117. Any opinions, findings, and conclusions or recommendations expressed in this material are those of the authors and do not necessarily reflect the views of NSF or EPA. We thank the MRL Central Facilities, which are supported by the MRSEC Program of the NSF under Award # DMR 1121053, and MEIAF, supported by the NSF under awards BES-9977772, DBI-0216480, and DEB-0444712.

## ■ REFERENCES

(1) Fu, F.; Dionysiou, D. D.; Liu, H. The use of zero-valent iron for groundwater remediation and wastewater treatment: A review. *J. Hazard. Mater.* **2014**, *267* (0), 194−205.

(2) O'Carroll, D.; Sleep, B.; Krol, M.; Boparai, H.; Kocur, C. Nanoscale zero valent iron and bimetallic particles for contaminated site remediation. *Adv. Water Resour.* **2013**, *51* (0), 104−122.

(3) Su, Y.; Adeleye, A. S.; Zhou, X.; Dai, C.; Zhang, W.; Keller, A. A.; Zhang, Y. Effects of nitrate on the treatment of lead contaminated groundwater by nanoscale zerovalent iron. *J. Hazard. Mater.* **2014**, *280* (0), 504−513.

(4) Adeleye, A. S.; Conway, J. R.; Garner, K.; Huang, Y.; Su, Y.; Keller, A. A. Engineered nanomaterials for water treatment and remediation: Costs, benefits, and applicability. *Chem. Eng. J.* **2016**, *286*, 640−662.

(5) Crane, R. A.; Dickinson, M.; Scott, T. B. Nanoscale zero-valent iron particles for the remediation of plutonium and uranium contaminated solutions. *Chem. Eng. J.* **2015**, *262* (0), 319−325.

(6) Mueller, N.; Braun, J.; Bruns, J.; Cernik, M.; Rissing, P.; Rickerby, D.; Nowack, B. Application of nanoscale zero valent iron (NZVI) for groundwater remediation in Europe. *Environ. Sci. Pollut. Res.* **2012**, *19* (2), 550−558.

(7) Comba, S.; Di Molfetta, A.; Sethi, R. A Comparison Between Field Applications of Nano-, Micro-, and Millimetric Zero-Valent Iron for the Remediation of Contaminated Aquifers. *Water, Air, Soil Pollut.* **2011**, *215* (1−4), 595−607.

(8) Su, C.; Puls, R. W.; Krug, T. A.; Watling, M. T.; O'Hara, S. K.; Quinn, J. W.; Ruiz, N. E. A two and half-year-performance evaluation of a field test on treatment of source zone tetrachloroethene and its chlorinated daughter products using emulsified zero valent iron nanoparticles. *Water Res.* **2012**, *46* (16), 5071−5084.

(9) Phenrat, T.; Saleh, N.; Sirk, K.; Kim, H.-J.; Tilton, R.; Lowry, G. Stabilization of aqueous nanoscale zerovalent iron dispersions by anionic polyelectrolytes: adsorbed anionic polyelectrolyte layer properties and their effect on aggregation and sedimentation. *J. Nanopart. Res.* **2008**, *10* (5), 795−814.

(10) Adeleye, A. S.; Keller, A. A.; Miller, R. J.; Lenihan, H. S. Persistence of commercial nanoscaled zero-valent iron (nZVI) and by-products. *J. Nanopart. Res.* **2013**, *15* (1), 1−18.

(11) Jiemvarangkul, P.; Zhang, W.-x.; Lien, H.-L. Enhanced transport of polyelectrolyte stabilized nanoscale zero-valent iron (nZVI) in porous media. *Chem. Eng. J.* **2011**, *170* (2−3), 482−491.

(12) Lv, X.; Xue, X.; Jiang, G.; Wu, D.; Sheng, T.; Zhou, H.; Xu, X. Nanoscale Zero-Valent Iron (nZVI) assembled on magnetic Fe3O4/graphene for Chromium (VI) removal from aqueous solution. *J. Colloid Interface Sci.* **2014**, *417* (0), 51−59.

(13) Shi, L.-n.; Zhang, X.; Chen, Z.-l. Removal of Chromium (VI) from wastewater using bentonite-supported nanoscale zero-valent iron. *Water Res.* **2011**, *45* (2), 886−892.

(14) Koutsospyros, A.; Pavlov, J.; Fawcett, J.; Strickland, D.; Smolinski, B.; Braida, W. Degradation of high energetic and insensitive munitions compounds by Fe/Cu bimetal reduction. *J. Hazard. Mater.* **2012**, *219−220* (0), 75−81.

(15) Su, Y.; Adeleye, A. S.; Huang, Y.; Sun, X.; Dai, C.; Zhou, X.; Zhang, Y.; Keller, A. A. Simultaneous removal of cadmium and nitrate in aqueous media by nanoscale zerovalent iron (nZVI) and Au doped nZVI particles. *Water Res.* **2014**, *63* (0), 102−111.

(16) Su, Y.; Adeleye, A. S.; Keller, A. A.; Huang, Y.; Dai, C.; Zhou, X.; Zhang, Y. Magnetic sulfide-modified nanoscale zerovalent iron (S-nZVI) for dissolved metal ion removal. *Water Res.* **2015**, *74* (0), 47−57.

(17) Kocur, C. M.; Chowdhury, A. I.; Sakulchaicharoen, N.; Boparai, H. K.; Weber, K. P.; Sharma, P.; Krol, M. M.; Austrins, L.; Peace, C.; Sleep, B. E.; O'Carroll, D. M. Characterization of nZVI Mobility in a Field Scale Test. *Environ. Sci. Technol.* **2014**, *48* (5), 2862−2869.

(18) Ševců, A.; El-Temsah, Y. S.; Joner, E. J.; Černík, M. Oxidative stress induced in microorganisms by zero-valent iron nanoparticles. *Microbes and Environments* **2011**, *26* (4), 271−281.

(19) Kim, E.-J.; Murugesan, K.; Kim, J.-H.; Tratnyek, P. G.; Chang, Y.-S. Remediation of Trichloroethylene by FeS-Coated Iron Nanoparticles in Simulated and Real Groundwater: Effects of Water Chemistry. *Ind. Eng. Chem. Res.* **2013**, *52* (27), 9343−9350.

(20) Su, Y.; Adeleye, A. S.; Huang, Y.; Zhou, X.; Keller, A. A.; Zhang, Y. Direct Synthesis of Novel and Reactive Sulfide-modified Nano Iron through Nanoparticle Seeding for Improved Cadmium-Contaminated Water Treatment. *Sci. Rep.* **2016**, *6*, 24358.

(21) Adeleye, A. S.; Keller, A. A. Long-term colloidal stability and metal leaching of single wall carbon nanotubes: effect of temperature and extracellular polymeric substances. *Water Res.* **2014**, *49* (0), 236−50.

(22) Adeleye, A. S.; Conway, J. R.; Perez, T.; Rutten, P.; Keller, A. A. Influence of Extracellular Polymeric Substances on the Long-Term Fate, Dissolution, and Speciation of Copper-Based Nanoparticles. *Environ. Sci. Technol.* **2014**, *48* (21), 12561−12568.

(23) Ma, S.; Zhou, K.; Yang, K.; Lin, D. Heteroagglomeration of Oxide Nanoparticles with Algal Cells: Effects of Particle Type, Ionic Strength and pH. *Environ. Sci. Technol.* **2015**, *49* (2), 932−939.

(24) Stevenson, L. M.; Dickson, H.; Klanjscek, T.; Keller, A. A.; McCauley, E.; Nisbet, R. M. Environmental Feedbacks and Engineered Nanoparticles: Mitigation of Silver Nanoparticle Toxicity to *Chlamydomonas reinhardtii* by Algal-Produced Organic Compounds. *PLoS One* **2013**, *8*(9), e7445610.1371/journal.pone.0074456

(25) Bolker, B. M. *Ecological Models and Data in R*; Princeton University Press: Princeton, NJ, 2008.

(26) Liu, A. R.; Liu, J.; Pan, B. C.; Zhang, W. X. Formation of lepidocrocite (gamma-FeOOH) from oxidation of nanoscale zero-valent iron (nZVI) in oxygenated water. *RSC Adv.* **2014**, *4* (101), 57377−57382.

(27) Zhang, W.-x.; Elliott, D. W. Applications of iron nanoparticles for groundwater remediation. *Remediation Journal* **2006**, *16* (2), 7−21.

(28) Wingender, J.; Neu, T.; Flemming, H. *Microbial Extracellular Polymeric Substances: Characterisation, Structure, and Function*; Springer, Berlin, 1999, p 123.

(29) Kadar, E.; Cunliffe, M.; Fisher, A.; Stolpe, B.; Lead, J.; Shi, Z. Chemical interaction of atmospheric mineral dust-derived nanoparticles with natural seawater — EPS and sunlight-mediated changes. *Sci. Total Environ.* **2014**, *468−469* (0), 265−271.

(30) Flemming, H.-C.; Neu, T. R.; Wozniak, D. J. The EPS matrix: the "house of biofilm cells. *J. Bacteriol.* **2007**, *189* (22), 7945−7947.

(31) Sutherland, I. W. Biofilm exopolysaccharides: a strong and sticky framework. *Microbiology* **2001**, *147* (1), 3−9.

(32) Mayer, C.; Moritz, R.; Kirschner, C.; Borchard, W.; Maibaum, R.; Wingender, J.; Flemming, H.-C. The role of intermolecular interactions: studies on model systems for bacterial biofilms. *Int. J. Biol. Macromol.* **1999**, *26* (1), 3−16.

(33) Pal, A.; Paul, A. Microbial extracellular polymeric substances: central elements in heavy metal bioremediation. *Indian J. Microbiol.* **2008**, *48* (1), 49−64.



DOI: 10.1021/acs.est.5b06251
*Environ. Sci. Technol.* 2016, 50, 5597−5605

(34) Giasuddin, A.; Kanel, S.; Choi, H. Adsorption of humic acid onto nanoscale zerovalent iron and its effect on arsenic removal. *Environ. Sci. Technol.* **2007**, *41* (6), 2022−2027.
(35) González, A. G.; Santana-Casiano, J. M.; González-Dávila, M.; Pérez-Almeida, N.; Suárez de Tangil, M. Effect of Dunaliella tertiolecta Organic Exudates on the Fe(II) Oxidation Kinetics in Seawater. *Environ. Sci. Technol.* **2014**, *48* (14), 7933−7941.
(36) Keenan, C. R.; Sedlak, D. L. Factors Affecting the Yield of Oxidants from the Reaction of Nanoparticulate Zero-Valent Iron and Oxygen. *Environ. Sci. Technol.* **2008**, *42* (4), 1262−1267.
(37) Reardon, E. J.; Fagan, R.; Vogan, J. L.; Przepiora, A. Anaerobic Corrosion Reaction Kinetics of Nanosized Iron. *Environ. Sci. Technol.* **2008**, *42* (7), 2420−2425.
(38) Moulder, J.; Stickle, W.; Sobol, P. E.; Bomben, K. *Handbook of X-ray Photoelectron Spectroscopy. A Reference Book of Standard Spectra for Identification and Interpretation of XPS Data*; Physical Electronics: Minnesota, MN, 1995.
(39) Baltrusaitis, J.; Cwiertny, D. M.; Grassian, V. H. Adsorption of sulfur dioxide on hematite and goethite particle surfaces. *Phys. Chem. Chem. Phys.* **2007**, *9* (41), 5542−5554.
(40) Reinsch, B. C.; Forsberg, B.; Penn, R. L.; Kim, C. S.; Lowry, G. V. Chemical Transformations during Aging of Zerovalent Iron Nanoparticles in the Presence of Common Groundwater Dissolved Constituents. *Environ. Sci. Technol.* **2010**, *44* (9), 3455−3461.
(41) Kadar, E.; Rooks, P.; Lakey, C.; White, D. A. The effect of engineered iron nanoparticles on growth and metabolic status of marine microalgae cultures. *Sci. Total Environ.* **2012**, *439* (0), 8−17.
(42) Keller, A. A.; Garner, K.; Miller, R. J.; Lenihan, H. S. Toxicity of Nano-Zero Valent Iron to Freshwater and Marine Organisms. *PLoS One* **2012**, *7* (8), e43983.
(43) García-Meza, J. V.; Barrangue, C.; Admiraal, W. Biofilm formation by algae as a mechanism for surviving on mine tailings. *Environ. Toxicol. Chem.* **2005**, *24* (3), 573−581.
(44) Chen, J.; Xiu, Z.; Lowry, G. V.; Alvarez, P. J. J. Effect of natural organic matter on toxicity and reactivity of nano-scale zero-valent iron. *Water Res.* **2011**, *45* (5), 1995−2001.
(45) Navarro, E.; Baun, A.; Behra, R.; Hartmann, N. B.; Filser, J.; Miao, A.-J.; Quigg, A.; Santschi, P. H.; Sigg, L. Environmental behavior and ecotoxicity of engineered nanoparticles to algae, plants, and fungi. *Ecotoxicology* **2008**, *17* (5), 372−386.



DOI: 10.1021/acs.est.5b06251
*Environ. Sci. Technol.* 2016, 50, 5597−5605